Deformation and Ductile Failure of a Low Alloyed Steel under High Strain Rate Loading

Shawky Abdel-Malek, Lothar W. Meyer, Norman Herzig

Nordmetall GmbH, Haupstraße 16, D-09221 Adorf/Erzgebirge, Germany

www.nordmetall.net, malek@nordmetall.net

Abstract:

It is well known that ductile failure of metal is occurring after a certain amount of plastic deformation. Therefore, knowledge about the deformation behavior of materials is required to understand damage processes and to describe the failure behavior using suitable constitutive equations. Thereby, the influence of temperature and strain rate has to be known for an accurate constitutive description of the mechanical behavior of metals.
Within this study, the MTS (Mechanical Threshold Stress) model is used for the description of the material behavior of low alloyed steels in a wide range of temperatures and strain rates. In addition, the model is extended using a new mathematical part to describe the effect of dynamic strain aging at low strain rates and high temperatures.
To describe the real material behavior, material data at high strains, high strain rates, and high temperatures are required, especially if the deformation and failure process is going to be simulated numerically. A new testing technique is used to perform stopped high rate tensile tests during necking process. Hence, the true stress and true strain behavior of the materials can be determined directly from high rate experiments and enhance the quality and accuracy of the parameter identification process for constitutive equations. By finite element calculations using LS-DYNA 3D, the tensile deformation of a specimen is simulated until crack initiation including necking and the stress triaxiality in the necking zone of a tensile specimen is evaluated. It is shown that the strain hardening characteristic of a material affects the development of stress triaxiality.

Keywords:

high strain rate, high plastic deformation, modeling, ductile failure.

1   Introduction

Mechanical testing gives information about material behavior at different temperatures and strain rates. The results are needed for the numerical analysis and the simulation of high strain rate deformation processes such as automobile crash test or high speed metal forming processes. For these processes the range of relatively high strains and very high strain rates is of great interest. In the high strain rate range, the flow stresses are influenced by the temperature increase during the deformation process. The major part of the deformation energy is transformed into heat leading to a reduction of the flow stress. A precise description of the material behavior needs not only a good agreement of the constitutive model with the experimental results at high strain rates, but also at high deformations. Dynamic strain aging will be active in a limited range of strain rate and temperature and leads to an enhancement of the flow stresses. This must be considered in the material model.

At ductile fractures, the material can fail due to the coalescence of voids, which occurs through three mechanisms: 1) squeezing of the matrix between voids, 2) nucleation and growth of secondary voids and 3) shearing between voids. Factors affecting the ductile failure are: stress state, temperature, strain rate, twin formation and dynamic strain aging. Understanding these effects allows to forecast, how and when failure occurs. This leads to a successful modeling of failure in a numerical simulation.

2   Material model

Accurate modeling of deformation processes of materials over a wide range of strain rates and temperatures requires a reliable constitutive description of the stress-strain behavior. Several physically and empirically based models have been developed for the use in computational codes [1]. Most models are using a constant strain hardening exponent n, which leads to higher flow stresses with increasing deformation. The MTS model "Mechanical Threshold Stress", which was developed by Follansbee et al. [2], is a physically based model. It is considering that the flow stress at a certain temperature and strain rate do not increase above a saturation stress. In the MTS model the flow stress is a sum of three parts: an athermal stress σ_a, the thermal stress σ_i for the interaction of dislocations with interstitial atoms and a threshold stress $\hat{\sigma}_\varepsilon$ for the dislocation/dislocation interaction:

$$\frac{\sigma}{\mu} = \frac{\sigma_a}{\mu_0} + S_i(\dot{\varepsilon}, T) \cdot \frac{\sigma_i}{\mu_0} + S_\varepsilon(\dot{\varepsilon}, T) \cdot \frac{\hat{\sigma}_\varepsilon}{\mu_0} \tag{1}$$

μ is the temperature dependent shear modulus and μ_0 is the shear modulus at 0 K. S_i and S_ε are factors expressing the effect of temperature and strain rate in a general form as:

$$S_{i,\varepsilon} = \left\{ 1 - \left[\frac{kT}{g_{0i,\varepsilon}\mu b^3} \ln\left(\frac{\dot{\varepsilon}_{0i,\varepsilon}}{\dot{\varepsilon}} \right) \right]^{1/q_{i,\varepsilon}} \right\}^{1/p_{i,\varepsilon}} \tag{2}$$

While σ_a and σ_i are taken as constants, the threshold stress $\hat{\sigma}_\varepsilon$ is a state parameter and treated differentially according to:

$$\theta = \frac{d\hat{\sigma}_\varepsilon}{d\varepsilon} = \theta_0(\dot{\varepsilon})\left(1 - \frac{\tanh\left(\alpha \dfrac{\hat{\sigma}_\varepsilon}{\hat{\sigma}_{\varepsilon s}(\dot{\varepsilon}, T)} \right)}{\tanh(\alpha)} \right) \tag{3}$$

where θ is the strain hardening and $\hat{\sigma}_{\varepsilon s}$ is the saturation stress. A detailed discussion of MTS model and how to determine the parameter is explained by Follansbee et al. [2-4].

At high temperatures or low strain rates the dynamic strain aging is affecting the flow stress. In order to consider this effect we suggest a forth stress part to be added to the MTS model. The equation (1) shall be written as:

$$\frac{\sigma}{\mu} = \frac{\sigma_a}{\mu_0} + S_i(\dot{\varepsilon},T) \cdot \frac{\sigma_i}{\mu_0} + S_\varepsilon(\dot{\varepsilon},T) \cdot \frac{\hat{\sigma}_\varepsilon}{\mu_0} + \frac{\sigma_{DSA}}{\mu} \tag{4}$$

where σ_{DSA} is a stress part, which results from the <u>D</u>ynamic <u>S</u>train <u>A</u>ging (DSA). It will be expressed with the following equation, so that it is only active in the region of the dynamic strain aging, figure 1.

$$\frac{\sigma_{DSA}}{\mu} = \frac{\sigma_{D0}}{\mu_0} \cdot \mathrm{sec}h\left[K_1 \cdot S_i(\dot{\varepsilon},T) - K_2\right] \tag{5}$$

σ_{D0}, K_1 und K_2 are constants, which will be determined by using the difference of experimental data σ_{exp} and the σ_{MTS} data calculated with equation (1).

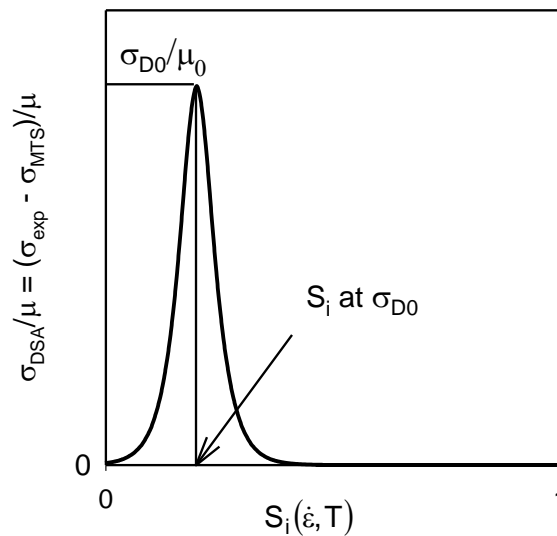$$\sigma_{DSA} = \sigma_{exp} - \sigma_{MTS} \tag{6}$$

Figure 1: Relationship between σ_{DSA} and $S_i(\dot{\varepsilon},T)$

3   Experimental procedures

Tension tests were carried out on a low alloyed tool steel under quasi-static and high rate loading conditions. Tensile tests at low and medium velocities were done with the proved 250 kN hydraulic test machine Instron 8503, which has a large test velocity range of v = 0.005 up to 800 mm/s.

Dynamic tensile tests were performed on the rotating wheel machine at different velocities, figure 2. The rotating wheel machine consists of a flywheel (200 kg) with a claw, which is released at the required test velocity and is impacting a yoke. The yoke pulls the test specimen, which is attached in a specimen holder. The force measurement is applied directly besides the gage length with strain gages. The strain was measured directly with strain gages. Because of high energy capacity of this apparatus, the test velocity is constant up to failure even for high strength, high ductile materials. For more details see Meyer et al. [5].
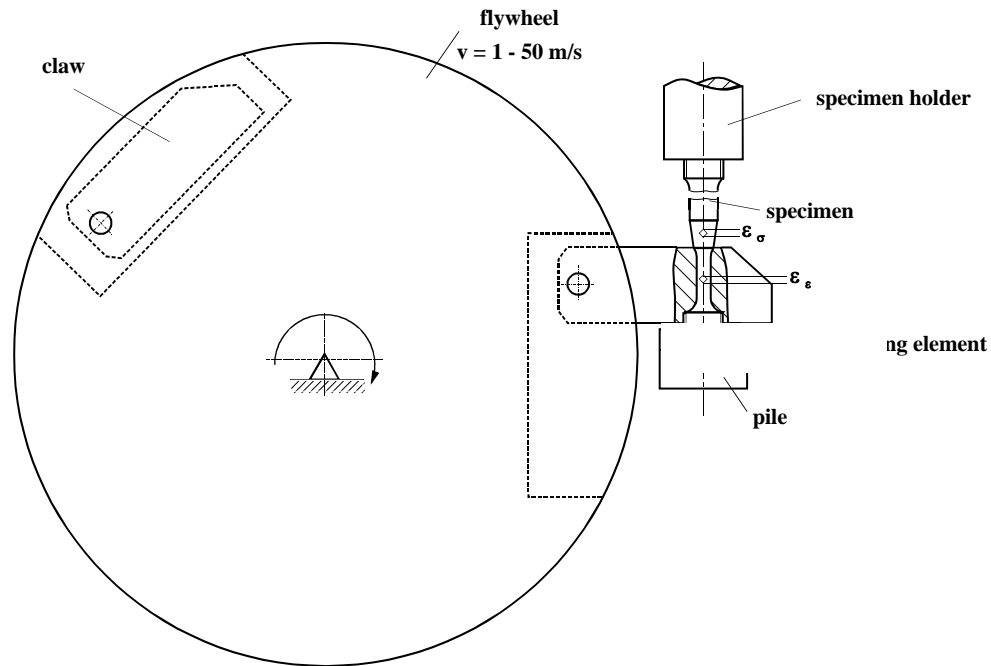
Figure 2: principle of high rate tensile testing with fly wheel setup

Only flow stresses up to UTS are used to get the parameter of the MTS model. To verify the material model at high deformations the high rate tensile test was interrupted in the necking region using a special stopping device. The stress is calculated from the measured force and the actual area of the smallest cross section and corrected to the uniaxial stress state according to Bridgman [6].

Characterization of the ductile failure behavior was performed by using notched specimens, which were tested under tensile loading with three speeds; v = 0.1 mm/s, 5 m/s and 25 m/s. The changes in the minimum diameter at the notch root were used as a criterion to measure the effective strain at failure.

4   Results and discussion

4.1   Modeling the flow stress

The parameters of the MTS model, eq. (1), were determined by using the results of the tension tests up to UTS in the strain rate range 10^{-4} s^{-1} to $5 \cdot 10^{3}$ s^{-1}. For high strain values, interrupted dynamic tensile tests were carried out with a test speed of 5 m/s. The required strain value is adjusted with a special device, which guides the deformation process into a secondary specimen, the so-called sacrifice specimen, which fails and remains the test specimen only deformed with a necking. The flow stress and strain are calculated with the actual force and cross sectional area and corrected to the uniaxial stress state according to Bridgman [6]. An advantage of this method is the considering of the adiabatic status resulting from the heating of the specimen under dynamic conditions.
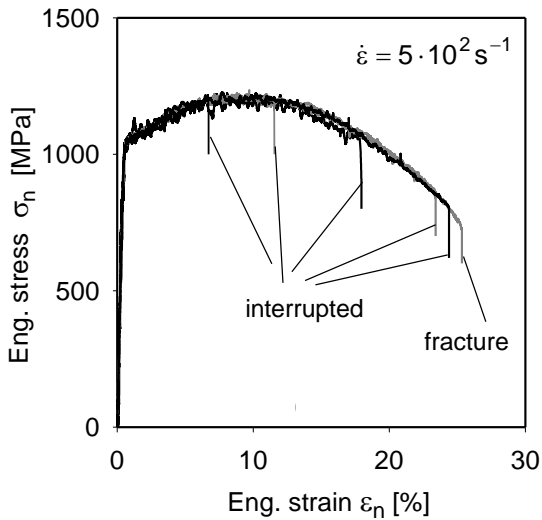
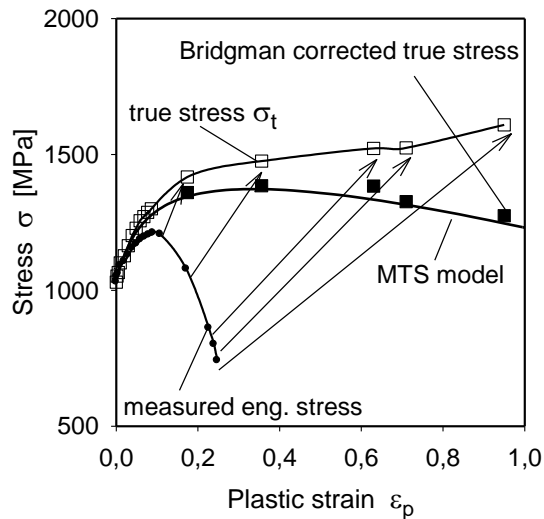*Figure 3: Stress strain diagrams of interrupted tests of low alloyed tool steel*

Figure 4: Comparison of experimental data and MTS model

Figure 3 shows the results of interrupted tensile tests of specimens with 10 mm gage length at a strain rate of $5 \cdot 10^2$ s^{-1} with a low scatter between six tests interrupted at certain stages of necking. The true stress was determined from the measured force and the true diameter in the necking zone and corrected for the uniaxial state according to Bridgman [6]. Comparing these results with the calculated curve of MTS model extrapolated from UTS to the fracture strain, a good agreement was achieved, Figure 4.

Figure 5 compares the experimental data at different strain rates with the calculated flow curves from the MTS model. Because of the effect of dynamic strain aging the experimental data at the strain rate of 10^{-3} s^{-1} reach higher values than the flow curve calculated with MTS model eq. (1). Considering the effect of dynamic strain aging by using the modified form of the MTS model eq. (4) a good agreement between the experimental data and the calculated curve (dashed curve) is resulting.

The calculated flow stresses with the modified MTS model eq. (4) are plotted in figure 6 as a function of the temperature at different strain rates. The effect of dynamic strain aging displaces to a higher temperature by a higher strain rate.
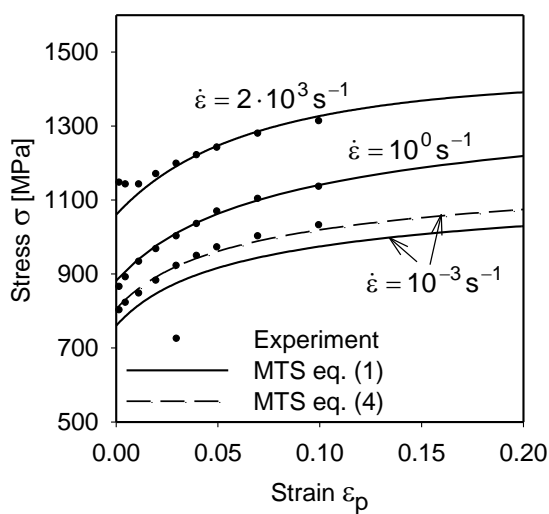

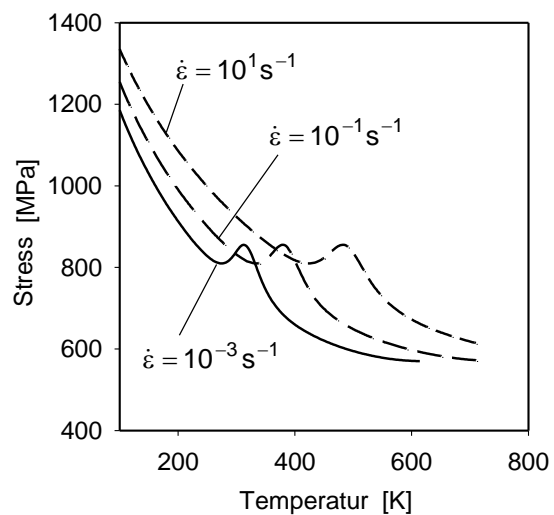*Figure 5: Influence of dynamic strain aging on the flow stress of a low alloyed tool steel*

Figure 6: Influence of dynamic strain aging at different temperatures and strain rates of a low alloyed tool steel

The sensitivity of the material to the dynamic strain aging can be measured with the value of the stress part σ_{D0}, the maximum of the stress due to dynamic strain aging σ_{DSA}. If the material is more sensitive to the temperature, the dynamic strain aging is increasing. In figure 6 the stress part σ_{D0} of the investigated steels is represented in dependence of the temperature softening in the temperature range of $50K \leq T \leq 300K$ at strain rates of $10^3 \, s^{-1}$. Obviously, the effect of dynamic strain aging of low alloyed steel is dependent on thermal activity of the material.

5   Ductile failure

Notched tensile specimens were used to get different stress states in characterizing the ductile failure of the investigated steel. The stress triaxiality must be determined at the fracture onset. Therefore, FEM computations were performed to calculate the development of the stress triaxiality σ_m/σ_v. The computations were carried out with LS-DYNA 3D explicit with 5 m/s and 25 m/s and also implicit to simulate the quasi-static loading. A quarter model is used for each notch radius and also for the unnotched specimen. The MTS model was used for the input of the material data.

To demonstrate the effect of strain hardening on the development of stress triaxiality, an implicit computation was carried out with a notch radius of 2.5 mm with two different flow curves. The first is an elastic-ideal plastic curve with $d\sigma/d\varepsilon = 0$, and the second presents elasticity followed by a strong linear strain hardening of $d\sigma/d\varepsilon = 500$ MPa. The yield stress (elastic limit) for both curves is 500 MPa. The results of these computations are that higher strain hardening yields to smaller stress triaxiality, figure 7.

The computed stress triaxiality of notched und unnotched specimens is presented in dependence of the equivalent strain, figure 8. The failure curve for quasi-static loading is represented by the dashed line. It is noticed that the stress triaxiality affects the failure behavior very much. This effect is well known in principle, but it is worth to recognize, how even moderate notch radii effectively reduce the ductility of a clean quality steel.
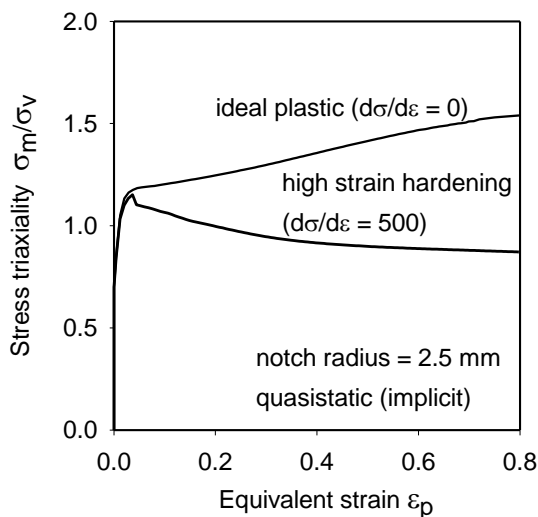

Figure 7: Influence of strain hardening on the stress triaxiality (FEM)
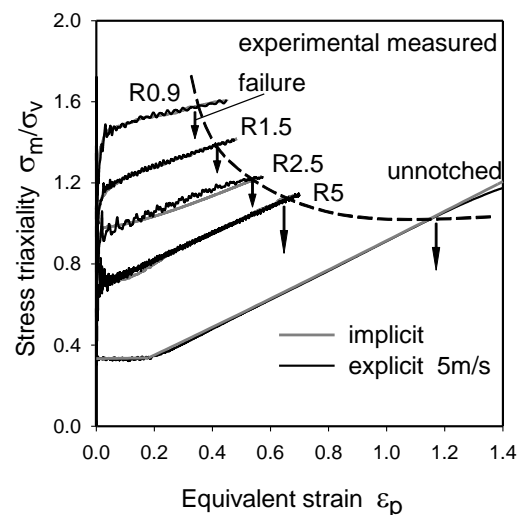
Figure 8: Stress triaxiality of different notch radius under quasi-static and dynamic loading (FEM)

The influence of strain rate on the effective fracture strain with this steel is moderate, see figure 9 for the unnotched and notched cases. With increasing strain rate the local fracture strain of unnotched specimens decreases lightly, up to $10^1 \, s^{-1}$, then it increases again clearly. In some metallic materials the so-called strain rate embrittlement [1,7] was observed. At high strain rate the ductility of metals can also increase due to the adiabatic heating resulting from the transformation of the deformation energy into heat. When the influence of the adiabatic heating is stronger than that of the strain rate, then the fracture strain increases at high strain rate. The local fracture strain of the notched specimens decreases slightly with increasing the strain rate. The stress triaxiality due to the notch retards the

strain across the area. That reduces the work available to be converted into heat, consequently, at high triaxialities no increase of the fracture strain at high rates can be observed, figure 9.

Adding to the before mentioned factors affecting the fracture strain, two additional factors play a role, the dynamic strain aging and the twin formation. The dynamic strain aging appears at low strain rate and reduces the fracture strain. Contrary, the twin formation occurs only at very high strain rates and enhances the fracture strain. A summary of these effects, figure 10, explains the possible reasons for the measured un-notched behavior shown in figure 9.
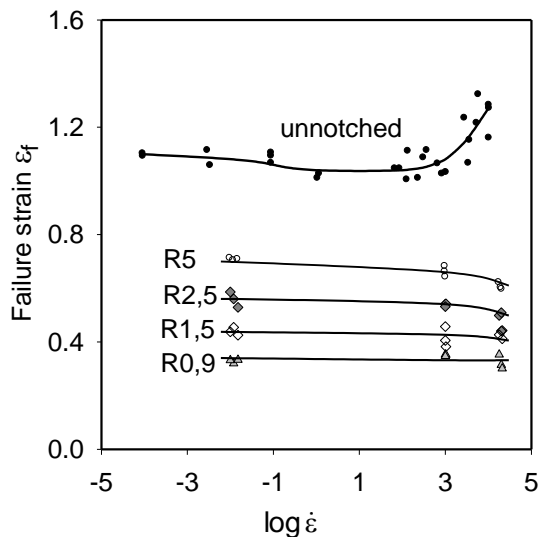

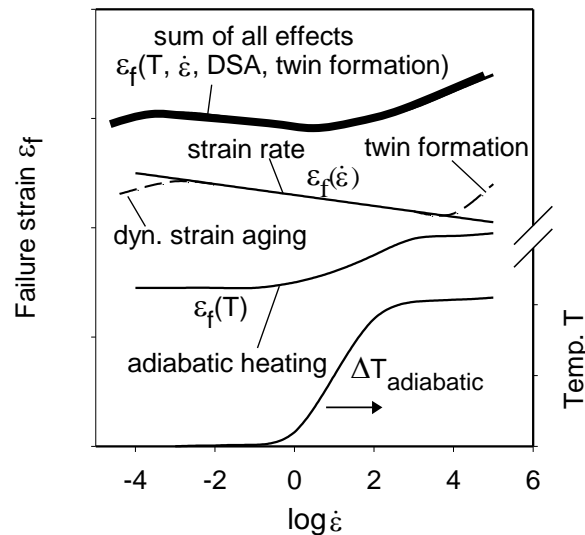*Figure 9: Dependence of the fracture strain on the strain rate*

Figure 10: Different effects on the failure strain in a wide range of strain rate

6   Conclusions

The material behavior of low alloy steel in a wide range of strain rate was described with the MTS model. Adding an extra stress part, the effect of the dynamic strain aging could be considered.
The damage curves of material can be determined using notched specimens in dependence of strain rate and temperature. The parameter of different failure models can be also estimated.
Many factors affecting the ductile failure are discussed and exemplarily represented.

7   References

[1]   Meyer, L. W.: Constitutive equations at high strain rate. In: Shock wave and high strain rate phenomena in materials, Eds.: Meyers, M. A.; Murr, L. E. and Staudhammer, K. P., Marcel Dekker, New Yourk, 1992, p.657-673.
[2]   Follansbee, P. S. and Kocks, U. F.: A constitutive description of the deformation of copper based on the use of the mechanical threshold stress as an internal state variable. Acta Metall., 36, 1988, p.81-93.
[3]   Follansbee, P. S. and Gray, G. T.: An analysis of the low temperature, low and high strain-rate deformation of Ti-6Al-4V. Metall. Trans., 20A, 1989, p.863-874.
[4]   Follansbee, P. S.; Huang, J. C. and Gray, G. T.: Low-temperature and high-strain-rate deformation of Nickel and Nickel-Carbon alloys and analysis of the constitutive behaviour according to an internal state variable model. Acta Metall., 38, 1990, p. 1241-1254.
[5]   Meyer, L. W.: Werkstoffverhalten hochfester Stähle unter einsinniger dynamischer Belastung. Dissertation, Universität Dortmund, 1982.
[6]   Bridgman, P. W.: The stress distribution at the neck of a tension specimen. Transactions of the A.S.M., 32, 1944, p.553-572.
[7]   Orava R. N.: The effect of dynamic strain rates on room temperature ductility. 1. Int. Conf. High Energy Forming, Estes Park, 110, 1967, p.183-188.